Quaternary Research 73 (2010) 336–350

Contents lists available at ScienceDirect

Quaternary Research

journal homepage: www.elsevier.com/locate/yqres

Palaeoenvironmental response to the ~74 ka Toba ash-fall in the Jurreru and Middle Son valleys in southern and north-central India

Sacha Claire Jones *

McDonald Institute for Archaeological Research, University of Cambridge, Downing Street, Cambridge, CB2 3ER, UK

ARTICLE INFO

Article history:
Received 26 February 2009
Available online 11 December 2009

Keywords:
Toba
Supereruption
India
Jurreru
Middle Son
Distal tephra
Palaeoenvironment

ABSTRACT

Distal deposits of rhyolitic volcanic ash from the ~74 ka "supervolcanic" eruption of Toba, in northern Sumatra, are preserved in numerous river valleys across peninsular India. The Toba eruption is hypothesized to have resulted in climate change and the devastation of ecosystems and hominin populations. This study reports the results of the analysis of sediments and stratigraphical sequences from sites in the Jurreru and Middle Son valleys in southern and north-central India. The aim of the study is to determine the extent of palaeoenvironmental change in both valleys as a result of the ash-fall. Inferences based on evidence from the Jurreru valley are more detailed, where pre- and post-Toba palaeoenvironmental changes are divided into seven phases. The results indicate that ash-fall deposits in both valleys underwent several phases of reworking that possibly lasted for several years, indicating that ash was mobile in the landscape for a considerable period of time prior to burial. This could have enhanced and lengthened the detrimental effects of the ash on vegetation and water sources, as well as animal and hominin populations.

Introduction

The ~74 ka "supereruption" of Toba, a "supervolcano" in northern Sumatra, was the largest eruption of the Quaternary period and one of the largest single explosive eruptions in Earth's history (Chesner and Rose, 1991), possessing a VEI of 8 or magnitude of $M = 8.8$ (Mason et al., 2004). In addition to at least 2000 km^3 of proximal ignimbrite deposits, Toba ejected more than 800 km^3 of the Youngest Toba Tuff (YTT), which covered at least 40,000,000 km^2 of southern and south-eastern Asia (Rose and Chesner, 1987). YTT deposits are preserved in river valley contexts across peninsular India (e.g., Westgate et al., 1998) and in Indian Ocean and South China Sea marine cores (Ninkovich et al., 1978; Pattan et al., 1999; Bühring et al., 2000; Schulz et al., 2002).

Academic and media interest in supervolcanoes and their supereruptions has grown considerably over the last decade, with several studies focusing on the human and environmental impacts that a supereruption may have when one occurs in the future (Sparks et al., 2005; Grattan, 2006; Self, 2006). Supereruptions are predicted to have far-reaching environmental impacts beyond the immediate vicinity of the volcano caused by the injection of vast quantities of gases and ash into the atmosphere. Sulphate aerosols, formed following the release of sulphur gases, are particularly hazardous. These can remain in the stratosphere for far longer than ash (years rather than months or days) and prevent light from reaching the Earth's surface. As a result, global climatic cooling is predicted to occur, possibly culminating in a "volcanic winter" (Rampino and Self, 1992). Climatic deterioration has been documented following a number of historical eruptions (e.g., Pinatubo, 1991); data from such eruptions have been used in climate modelling studies to predict the effects of a supereruption on global climate (e.g., Jones et al., 2005). In addition to the negative impacts of global cooling and decreased solar radiation on vegetation (but see Gu et al. (2003) who argue for increased photosynthesis under more diffuse light conditions), the coverage of continent-sized areas in volcanic ash must also be considered. White ash, together with increased snow and decreased vegetation cover, may all contribute to the albedo effect, backscattering incoming radiation and perpetuating global cooling. Ash can also have detrimental impacts on terrestrial (e.g., Dale et al., 2005) and aquatic habitats (e.g., Riedel et al., 2001) and on animal (e.g., Cronin et al., 1998) and human health (Horwell and Baxter, 2006); however, the extent of these impacts can be highly variable. In fact, caution is recommended against the often automatic assumption that supereruptions have catastrophic consequences (Grattan, 2006). Some regions may suffer from both ash-fall and climate change, yet others may experience only the latter. These factors, together with the assumption that not all ecosystems are equally vulnerable to environmental change, mean that the speed of recovery following a supereruption may exhibit considerable regional variation. Supereruptions are very rare events, with one estimated to occur every 100,000–200,000 yr (Self, 2006). Therefore, in order to understand the nature and extent of their impacts, we are currently reliant on information from global climatic modelling studies combined with that from palaeoclimatic, palaeoenvironmental and archaeological investigations of past supereruptions, such as the YTT event.

* Fax: +44 1223 333536.
E-mail address: scj23@cam.ac.uk.

0033-5894/$ – see front matter © 2009 University of Washington. Published by Elsevier Inc. All rights reserved.
doi:10.1016/j.yqres.2009.11.005

The ~74 ka Toba eruption injected massive quantities of volcanic gases and ash into the stratosphere and is hypothesized to have induced a ~6-yr-long volcanic winter (Rampino and Self, 1992) and accelerated and worsened stadial conditions during the ~1000 yr in between Dansgaard–Oeschger (D-O) events 19 and 20. This is supported by evidence from the GISP 2 ice core in Greenland, where a 6-yr-long sulphate peak has been linked to the Toba eruption (Zielinski et al., 1996; but see Oppenheimer, 2002). Ecosystems and *Homo sapiens* populations are argued to have been devastated as a result (Ambrose, 1998). Other studies, however, have argued against severe post-Toba climatic deterioration (Oppenheimer, 2002), as well as any considerable impacts on animal populations (e.g., Gathorne-Hardy and Harcourt-Smith, 2003). Furthermore, an analysis of pre- and post-Toba lithic artefact assemblages from the Jurreru valley in southern India, an area directly affected by the Toba ash-fall, shows technological continuity post-Toba, suggesting persistence of hominin populations after the eruption (Petraglia et al., 2007).

Toba's impact on palaeoclimate has been examined through analyses of marine core sediments that preserve YTT (Schulz et al., 2002; Huang et al., 2001) and predictive modelling of global climate change following a "supereruption" (e.g., Bekki et al., 1996; Jones et al., 2007; Robock et al., 2009). However, prior studies have not investigated the impacts of the YTT ash-fall or possible post-eruption climate change on terrestrial habitats in India. The preservation of YTT in stratified contexts throughout India offers an excellent data source with which to reconstruct the local and regional palaeoenvironmental consequences of the Toba eruption. Using these data, inferences can also be made regarding the impact of palaeoenvironmental change on hominin populations (Jones, 2007a, 2007b). Addressing these issues, this paper presents the results of the analysis of sediments and stratigraphic sequences from the Jurreru and Middle Son river valleys, located in southern and north-central India, respectively. The results of particle size, magnetic susceptibility and loss on ignition analyses of sediment and tephra samples are used to infer geomorphological changes following the Toba ash-fall. Evidence from the Jurreru valley is discussed in the greatest detail, having been subjected to more intensive and extensive fieldwork and sampling. Combining sedimentological data and stratigraphic observations, conclusions are made regarding the impacts of the Toba ash-fall on habitats in both valleys.

Study areas

Jurreru valley

Extensive deposits of Toba ash, up to ~2.5 m thick, are preserved in the Jurreru river valley (15°19.33′N; 78°8.02′E), one of several valleys that cut through the Erramala Hills in Kurnool District of Andhra Pradesh (Fig. 1A). The Jurreru ash deposits have been mined by local villagers for approximately 30 yr, leaving numerous small quarries that reveal vertical exposures of ash located throughout the valley (Fig. 2A). Measurement of ash thickness (ranging from 0.15 to 2.55 m thick) at 204 locations indicates that >0.64 km^2 of the valley was buried by $\sim 7 \pm 0.7 \times 10^5$ m^3 of ash (Petraglia et al., 2007).

Numerous archaeological sites have been recorded in the valley, ranging from the Lower Palaeolithic through to Historical periods. Archaeological excavations of Upper Pleistocene contexts have been conducted at several open-air and rockshelter sites (Petraglia et al., 2009). Samples used in this study were restricted to excavated trenches that preserve the YTT layer (localities 3, 21 and the Dry Well). Optically stimulated luminescence (OSL) dates provide ages for pre- and post-Toba sediments and lithic artefacts from localities 3 and 21. Artefacts excavated from 1 to 1.5 m beneath the ash at locality 3 are dated to less than 77 ± 6 ka (JLP3A-200), and post-Toba artefacts at the same locality in a context ~1.1 m above the ash are dated to 74 ± 7 ka (JLP3-380) (Petraglia et al., 2007). The first post-Toba artefacts at locality 21, discovered only ~30 cm above the ash, are dated to 38 ± 3 ka (JLP21B-30) (Petraglia et al., 2009). Sediment samples were taken from pre- and post-ash contexts at localities 3 and the Dry Well, within-ash samples were restricted to locality 3, and post-ash samples were taken from localities 3, 21 and the Dry Well.

Middle Son valley

The middle reaches of the Son river, located in north-eastern Madhya Pradesh, are bordered by the topographically prominent Kaimur range to the north and the hills of the Baghelkhand Plateau to the south (Fig. 1C). Extensive Quaternary alluvial deposits are preserved in the Middle Son, traceable for ~70 km from west (Chorat) to east (Bichhi) and running northwards to the foot of the Kaimur Hills (Williams and Royce, 1982). The modern-day course of the river Son and its tributaries have incised these deposits, creating numerous cliff sections, some ~38 m high. Archaeological and geological research has been conducted in the Middle Son valley since the 1960s. This has resulted in the discovery of numerous Lower Palaeolithic to Neolithic archaeological sites (Sharma and Clark, 1983), and the creation of geomorphological models that hypothesize the sequence of deposition of Pleistocene and Holocene sediments in the valley (Williams and Royce, 1982; Williams et al., 2006).

The first Toba tephra deposits of India were discovered in the Middle Son in 1980 (Williams and Royce, 1982), later geochemically characterised as YTT (Rose and Chesner, 1987). YTT occurs as discontinuous beds that extend over a distance of ~30 km; typical exposures are described at Ghoghara, Khuteli, Ramnagar and Nakjhar (Basu et al., 1987). In this study, sections were cut through the ash layer and part of the underlying and overlying deposits at Khuteli (24°32.48′N; 82°16.55′E) and Ghoghara (24°30.12′N; 82°1.05′E) (Fig. 2E). Sediment samples were collected from both section cuttings. At both localities, situated ~30 km apart and on opposite banks of the Son, the steep cliff sections are subjected to erosional forces during each monsoon season (Fig. 2D). As a result, pre-ash deposits are obscured by massive talus sands at both sites, and, in places, post-ash deposits are similarly obscured. The ash is relatively resistant to erosion when compared to the overlying and underlying fluvial sands and gravels, however, blocks of YTT are often encountered downslope of their primary context due to erosion and collapse.

Methods

Magnetic susceptibility, particle size and loss on ignition data were obtained for 46 sediment samples from localities 3, 21 and the Dry Well in the Jurreru, and 14 from Khuteli and Ghoghara in the Middle Son. The sampling strategy was dictated by changes in stratigraphy rather than regular sampling at evenly spaced intervals. The magnetic susceptibility of discrete sediment samples (10 cm^3) was measured using a Bartington magnetic susceptibility MS2 meter and MS2B dual frequency sensor. The particle size distribution of all samples was determined using a Malvern Mastersizer 2000 laser diffraction particle size analyzer. All analyses were conducted in the Physical Geography Laboratories in the Department of Geography at the University of Cambridge.

Results

Table 1 reports particle size, magnetic susceptibility and loss on ignition data for all samples (see supplementary MS Excel file for the full particle size dataset). A proportion of these data are displayed alongside section drawings (Figs. 3–6). Several important stratigraphic features encountered during excavations of the locality 3 ash layer are reported, as are key characteristics of the Middle Son sections.

https://doi.org/10.1016/j.yqres.2009.11.005 Published online by Cambridge University Press

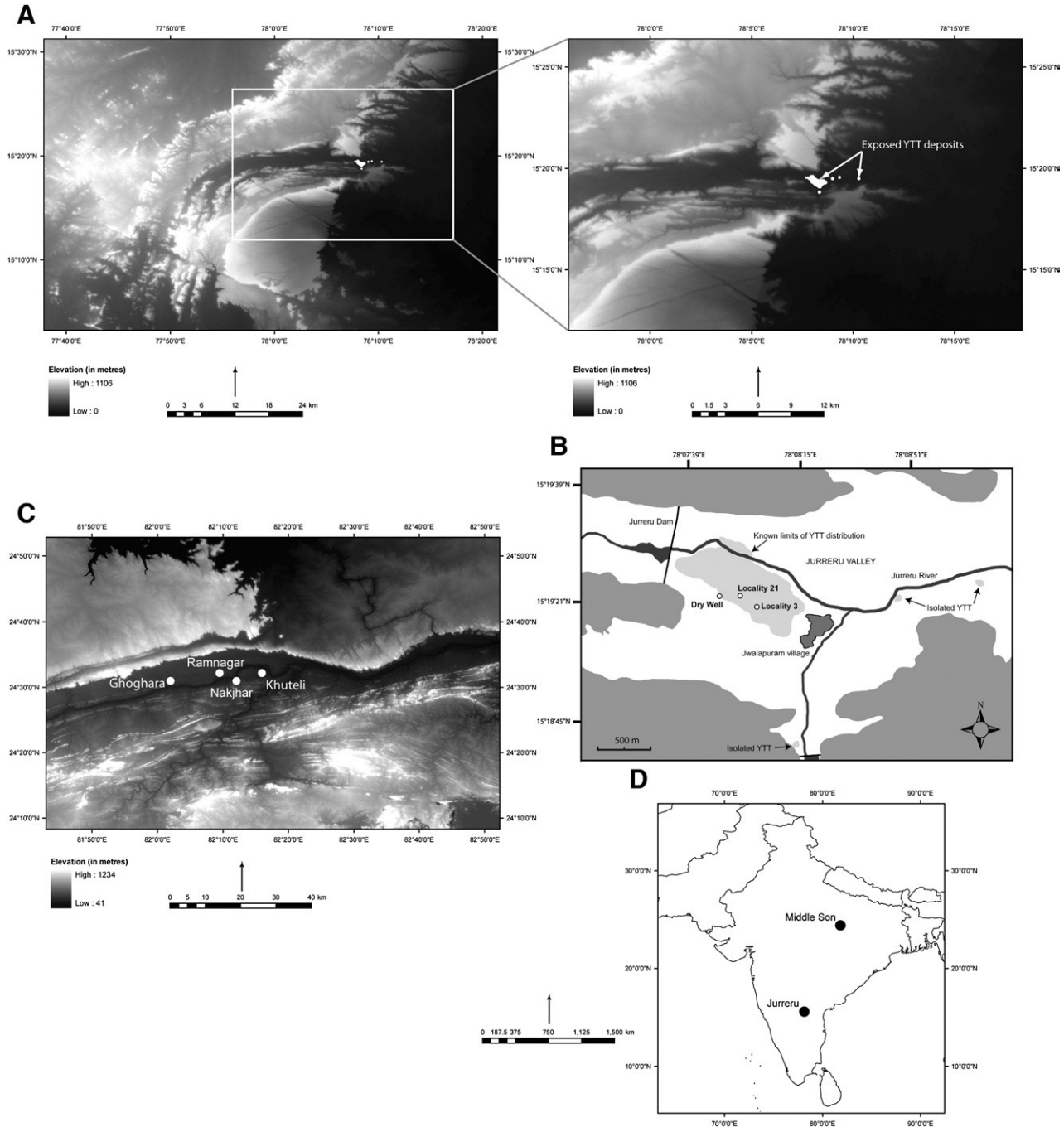

Figure 1. (A) The location and extent of YTT deposits in the Jurreru river valley; (B) sampled localities in the Jurreru valley; (C) Middle Son valley YTT deposits (white circles) at the sites of Ghoghara, Ramnagar, Nakjhar and Khuteli; (D) the location of the Jurreru and Middle Son valleys in India.

Macroscopic features preserved within the Jurreru valley YTT deposits

Excavation of the ~2.55-m-thick ash layer at locality 3 revealed several features preserved within the ash (Petraglia et al., 2007, 2009). Some of these features have also been observed within the ash at other localities in the valley. The most abundant of these include fossilized plant remains (e.g., roots and stems) and insect burrows. Some are *in situ* and extend vertically through the ash (Fig. 7A, B). Most, however, are fragmentary and are not preserved in their original growth positions (Fig. 8F). Not only do these fossils exhibit varied morphologies but they also present different states of preservation; some are pale grey and lithified, most probably by silica and carbonate, yet others are unfossilized and possess a brown-grey woody appearance. Some large examples of the latter have been encountered that possibly represent the branches or trunks of shrubs or trees (Figs. 8E, G). A proportion of these lithified and unlithified structures represent small animal burrows (e.g., rodents, insects, crustaceans, worms). Termite nests are encountered within the ash, as are a variety of other types of nests or burrows; some are clearly fossilized and some preserve the former structure of the internal burrow chambers (Figs. 7C, E). Others are unlithified sediment-filled structures that appear to be animal- rather than plant-derived, possibly representing termitaria (Fig. 7D). Living roots and relatively recent burrowing structures are also visible, representing a post-depositional intrusion into the ash.

Five grey horizontal hardpans (~1–10 mm thick) are preserved within the locality 3 ash, representing the termination of a series of

https://doi.org/10.1016/j.yqres.2009.11.005 Published online by Cambridge University Press

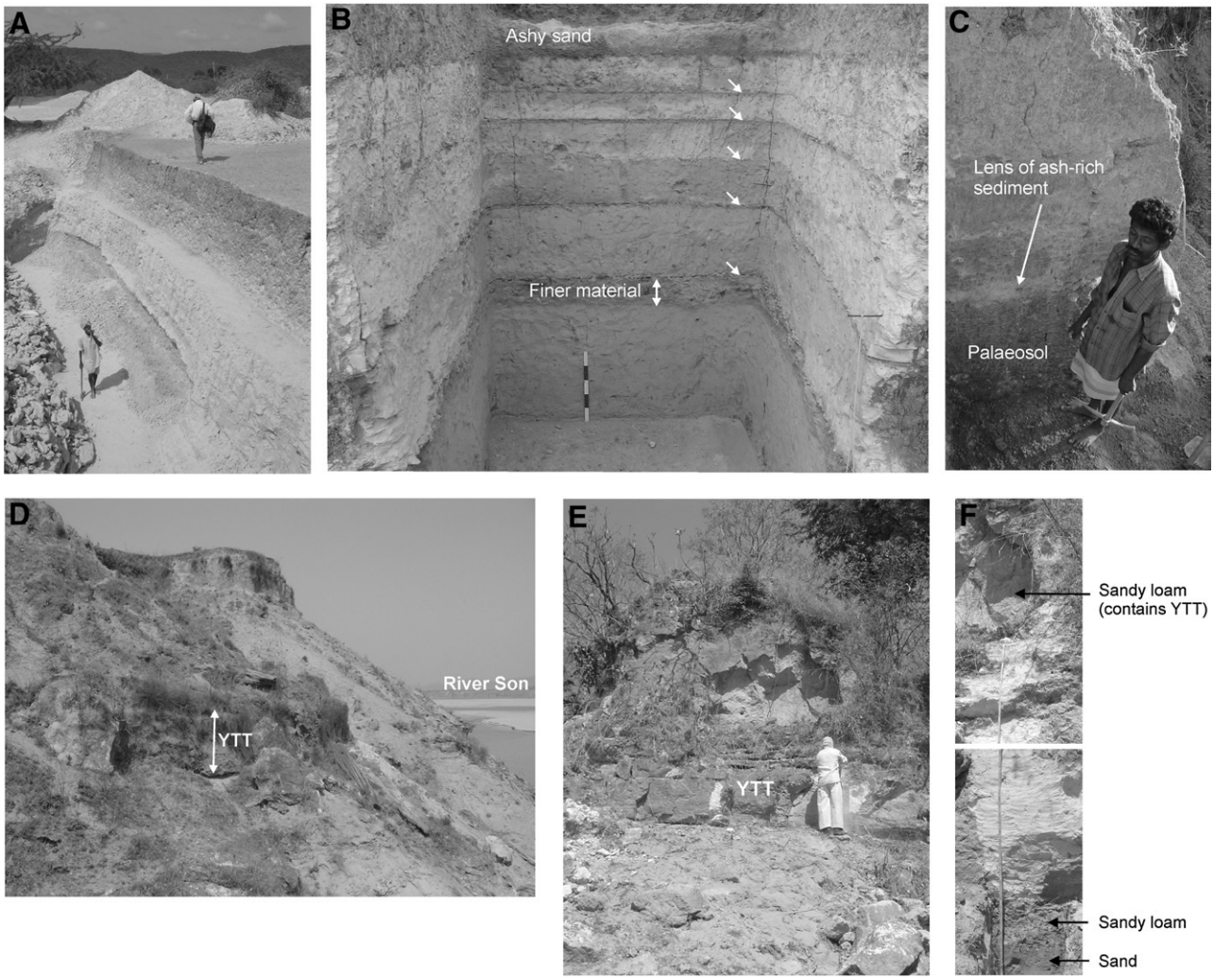

Figure 2. (A) ~2.5-m-thick YTT deposits visible in a mined quarry in the Jurreru valley; (B) excavated trench at locality 3 (Jurreru valley). Five horizontal hardpans (white arrows) are preserved within the 2.5 m of redeposited YTT. A fining upwards sequence during the first ash redeposition event is clearly visible (scale bar = 50 cm); (C) reworked YTT overlying a palaeosol in the Dry Well section cutting, located ~370 m to the north-west of locality 3; (D) YTT deposits in Khuteli cliff section on the southern bank of the river Son, Middle Son valley; (E) YTT deposits at Ghoghara (northern bank of the river Son); (F) Ghoghara section cutting.

fining-upwards sequences (Fig. 2B). These hardpans are continuous throughout the quarry walls at locality 3, yet in some other quarries, the hardpans are discontinuous and relatively indistinct. Excavation exposed the surfaces of all hardpans and revealed several interesting features. These include horizontally-oriented traces of either large roots or burrows, particularly visible across the surface of the lowermost hardpan. Filled-in mudcracks are also visible in both horizontal and vertical exposures (Figs. 8C, D). In plan view, small and intricate rootlet traces are present on the hardpan, as are patterns of black speckling that were possibly formed as a result of Fe-Mn staining or microbial activity.

A distinct ~5 cm layer of volcanic ash is visible at the base of the locality 3 tephra, forming a sharp boundary with the underlying orange-brown silt. This ash is more compact and slightly darker than the overlying tephra (Fig. 8B). The junction between the two deposits is also marked by a very thin (<1 mm) and discontinuous layer of orange-brown sediment and, in some areas, by occasional pellet-like structures. In places, soft sediment deformation structures, originating from the underlying sediment, intrude into this ash layer (Fig. 8A). This distinct layer may represent primary ash fallout. This is supported by the presence of primary ash layers of comparable thickness preserved in Indian Ocean marine cores. None of the aforementioned features have previously been documented in any other Toba ash deposits, and references to similar structures in distal ash deposits from other eruptions have yet to be encountered.

Key features of the ash and associated sediments at Khuteli and Ghoghara in the Middle Son valley

At Khuteli, small calcium carbonate concretions are present in low concentrations throughout the ash but are more common in the upper 50 cm. No additional macroscopic sedimentological features are visible within the ash. The colour of the ash changes from very pale brown (10YR 7/3 dry) at the base to light yellowish brown (10 YR 6/4) in the upper levels. *In situ* large horizontally oriented calcium carbonate-cemented sand structures directly overlie the ash. Yellow-brown sands overlie and underlie the ash; horizontally and cross-bedded laminated sands are visible in the vicinity of the section cutting and appear to both stratigraphically pre- and post-date the ash layer.

At Ghoghara, 50 cm of pre-tephra sediment was exposed, consisting of two different deposits; ~28 cm of yellowish brown (10YR 5/4 dry) sandy loam immediately underlies the ash and loose yellowish brown (10YR 5/4 dry) sand lies beneath this. The ash becomes progressively less pure as height above the base of the ash increases. The lowermost ~80 cm of the ash unit consists of relatively pure and compact very pale brown (10YR 8/2 dry) tephra. Above this,

https://doi.org/10.1016/j.yqres.2009.11.005 Published online by Cambridge University Press

Table 1
Sample descriptions, magnetic susceptibility (MS) and loss on ignition data for sediment samples from sites in the Jurreru and Middle Son valley. Particle size distributions for each sample is available as supplementary data.

Site	Sample	Height above base of ash (cm)	Texture	Sorting	Skewness	MS (10^{-8} m^3/kg)[a]	% Organic[b]	% $CaCO_3$[b]
Dry well	JWP DW 01	−65.0	Silt loam	Very poorly sorted	Fine skewed	131.6	1.112	15.663
Dry well	JWP DW 02	−5.0	Loamy sand	Very poorly sorted	Strongly coarse skewed	51.5	1.150	11.089
Dry well	JWP DW 03	10.0	Sandy loam	Very poorly sorted	Fine skewed	90.8	2.200	6.059
Dry well	JWP DW 04	15.0	Silt loam	Poorly sorted	Coarse skewed	101.7	2.341	5.861
Dry well	JWP DW 05	20.0	Silt loam	Very poorly sorted	Symmetrical	191.9	1.110	12.119
Dry well	JWP DW 07	35.0	Silt	Poorly sorted	Symmetrical	182.4	1.013	16.555
JWP 21	JWP 21-01	2.5[c]	Silt loam	Poorly sorted	Coarse skewed	53.5	3.467	1.627
JWP 21	JWP 21-02	7.5[c]	Silt loam	Poorly sorted	Symmetrical	61.7	3.285	4.280
JWP 21	JWP 21-08	30.0[c]	Silt loam	Poorly sorted	Coarse skewed	148.3	1.956	14.471
JWP 21	JWP 21-03	40.0[c]	Sandy loam	Very poorly sorted	Coarse skewed	174.1	2.237	16.718
JWP 21	JWP 21-04	52.5[c]	Sandy loam	Very poorly sorted	Strongly coarse skewed	153.5	1.121	18.194
JWP 21	JWP 21-05	75.0[c]	Loamy sand	Very poorly sorted	Strongly coarse skewed	155.5	1.129	19.119
JWP 21	JWP 21-06	113.0[c]	Silt loam	Very poorly sorted	Fine skewed	150.9	1.168	10.535
JWP 21	JWP 21-07	165.0[c]	Silt loam	Very poorly sorted	Strongly fine skewed	54.8	1.986	18.233
JWP 3A	JWP 3A 09	−130.0	Silt loam	Very poorly sorted	Fine skewed	66.2	1.074	27.428
JWP 3	JWP 3 SS16	−87.0	Silt	Poorly sorted	Fine skewed	136.6	1.673	13.226
JWP 3	JWP 3A 10	−70.0	Silt	Poorly sorted	Symmetrical	123.4	1.191	9.841
JWP 3	JWP 3 SS15	−62.0	Silt loam	Very poorly sorted	Fine skewed	119.3	1.586	8.827
JWP 3	JWP 3 SS14	−30.0	Silt	Poorly sorted	Symmetrical	106.9	1.612	10.175
JWP 3	JWP 3 SS13	−10.0	Silt loam	Very poorly sorted	Fine skewed	66.1	1.673	11.038
JWP 3	JLP3-01S	−10.0	Silt	Poorly sorted	Fine skewed	84.2	1.397	13.049
JWP 3	JWP3-02C	0.0	Silt loam	Poorly sorted	Coarse skewed	54.9	3.683	1.591
JWP 3	JLP3-19S	20.0	Silt loam	Poorly sorted	Coarse skewed	40.2	3.526	1.420
JWP 3	JWP3-05C	62.5	Silt loam	Poorly sorted	Coarse skewed	40.4	3.590	1.588
JWP 3	JLP3-04S	74.5	Silt loam	Poorly sorted	Coarse skewed	40.3	3.515	3.867
JWP 3	JWP3-06C	87.5	Silt	Poorly sorted	Coarse skewed	81.2	3.625	2.009
JWP 3	JWP3-11C	100.0	Silt loam	Very poorly sorted	Fine skewed	101.4	3.586	6.636
JWP 3	JWP3-07C	130.0	Silt loam	Poorly sorted	Coarse skewed	41.2	3.530	1.230
JWP 3	JWP3-E09	150.0	Silt	Poorly sorted	Fine skewed	84.5	3.128	12.052
JWP 3	JWP3-08C	170.0	Silt loam	Poorly sorted	Symmetrical	41.4	3.500	1.447
JWP 3	JWP3-E07	178.0	Silt loam	Poorly sorted	Symmetrical	47.5	2.363	22.150
JWP 3	JLP3-09S	182.5	Sandy loam	Poorly sorted	Coarse skewed	42.1	3.213	3.327
JWP 3	JWP3-E04	200.0	Silt loam	Poorly sorted	Fine skewed	83.9	2.251	27.935
JWP 3	JLP3-10S	207.5	Silt loam	Poorly sorted	Coarse skewed	42.2	3.192	2.333
JWP 3	JWP3-E02	216.0	Silt	Poorly sorted	Symmetrical	43.9	2.845	22.250
JWP 3	JLP3-12S	230.0	Silt loam	Poorly sorted	Symmetrical	39.9	3.447	6.369
JWP 3	JWP3-E01	240.0	Silt	Poorly sorted	Symmetrical	52.2	2.385	46.302
JWP 3	JWP3-14C	250.0	Sandy loam	Poorly sorted	Coarse skewed	86.8	2.831	6.282
JWP 3	JLP3-15S	290.0	Loamy sand	Very poorly sorted	Coarse skewed	139.4	2.030	13.055
JWP 3	JWP 3 SS07	302.0	Sand	Poorly sorted	Strongly coarse skewed	87.1	0.535	9.913
JWP 3	JWP 3 SS06	313.0	Sand	Poorly sorted	Strongly coarse skewed	101.1	0.539	8.582
JWP 3	JWP 3 SS05	325.0	Sandy loam	Very poorly sorted	Strongly coarse skewed	112.0	0.675	13.537
JWP 3	JWP 3 SS04	334.0	Sand	Poorly sorted	Strongly coarse skewed	120.7	0.684	10.013
JWP 3	JLP3-16S	345.0	Sand	Poorly sorted	Coarse skewed	98.5	0.637	7.307
JWP 3	JWP 3 SS03	354.0	Loamy sand	Very poorly sorted	Strongly coarse skewed	118.4	0.722	10.911
JWP 3	JWP 3 SS02	370.0	Sand	Poorly sorted	Strongly coarse skewed	117.9	1.075	9.056
JWP 3	JWP 3 SS01	383.0	Silt loam	Very poorly sorted	Symmetrical	111.2	1.892	12.247
Khuteli	KTL-SS-01	−65.0	loamy sand	Poorly sorted	Strongly coarse skewed	106.3	1.241	2.403
Khuteli	KTL-SS-02	−5.0	loamy sand	Very poorly sorted	Strongly coarse skewed	106.8	0.897	2.766
Khuteli	KTL-SS-03	20.0	Silt loam	Poorly sorted	Symmetrical	41.8	3.367	3.473
Khuteli	KTL-SS-04	85.0	Silt loam	Poorly sorted	Coarse skewed	53.0	2.956	4.047
Khuteli	KTL-SS-05	150.0	Sandy loam	Poorly sorted	Symmetrical	133.8	1.837	17.697
Khuteli	KTL-SS-06	235.0	Sandy loam	Very poorly sorted	Coarse skewed	141.2	1.485	5.208
Ghoghara	GGR-SS-01	−40.0	Sand	Moderately well sorted	Coarse skewed	47.4	0.241	0.671
Ghoghara	GGR-SS-02	−15.0	Sandy loam	Very poorly sorted	Coarse skewed	42.6	1.058	3.829
Ghoghara	GGR-SS-03	25.0	Silt loam	Poorly sorted	Symmetrical	65.1	3.680	4.848
Ghoghara	GGR-SS-04	65.0	Sandy loam	Poorly sorted	Coarse skewed	15.0	3.169	3.188
Ghoghara	GGR-SS-05	90.0	Sandy loam	Poorly sorted	Symmetrical	55.5	2.400	4.158
Ghoghara	GGR-SS-06	115.0	Loamy sand	Poorly sorted	Symmetrical	23.1	1.763	7.075
Ghoghara	GGR-SS-07	160.0	Loamy sand	Poorly sorted	Strongly coarse skewed	62.2	1.107	5.622
Ghoghara	GGR-SS-08	235.0	Sandy loam	Poorly sorted	Symmetrical	160.4	2.410	3.671

[a] Mass specific magnetic susceptibility (low frequency) (SI units 10^{-8} m^3/kg).
[b] Dry weight.
[c] Height above the upper surface of the ash.

the non-tephra component suddenly increases as indicated by a colour change; however, the ash is still the dominant constituent. This continues for the next 95 cm, where small irregular calcium carbonate concretions appear in the final ~35 cm. At ~1.75 m above the base of the ash, a horizontal erosional ledge exists, probably marking a temporal break in deposition. Ash is still present in the ~2 m of deposit that overlies this.

Discussion

Phases of palaeoenvironmental change in the Jurreru valley before, during and after the Toba ash-fall

Seven broad phases of palaeoenvironmental change in the Jurreru valley are proposed here; these are based on information gathered

https://doi.org/10.1016/j.yqres.2009.11.005 Published online by Cambridge University Press

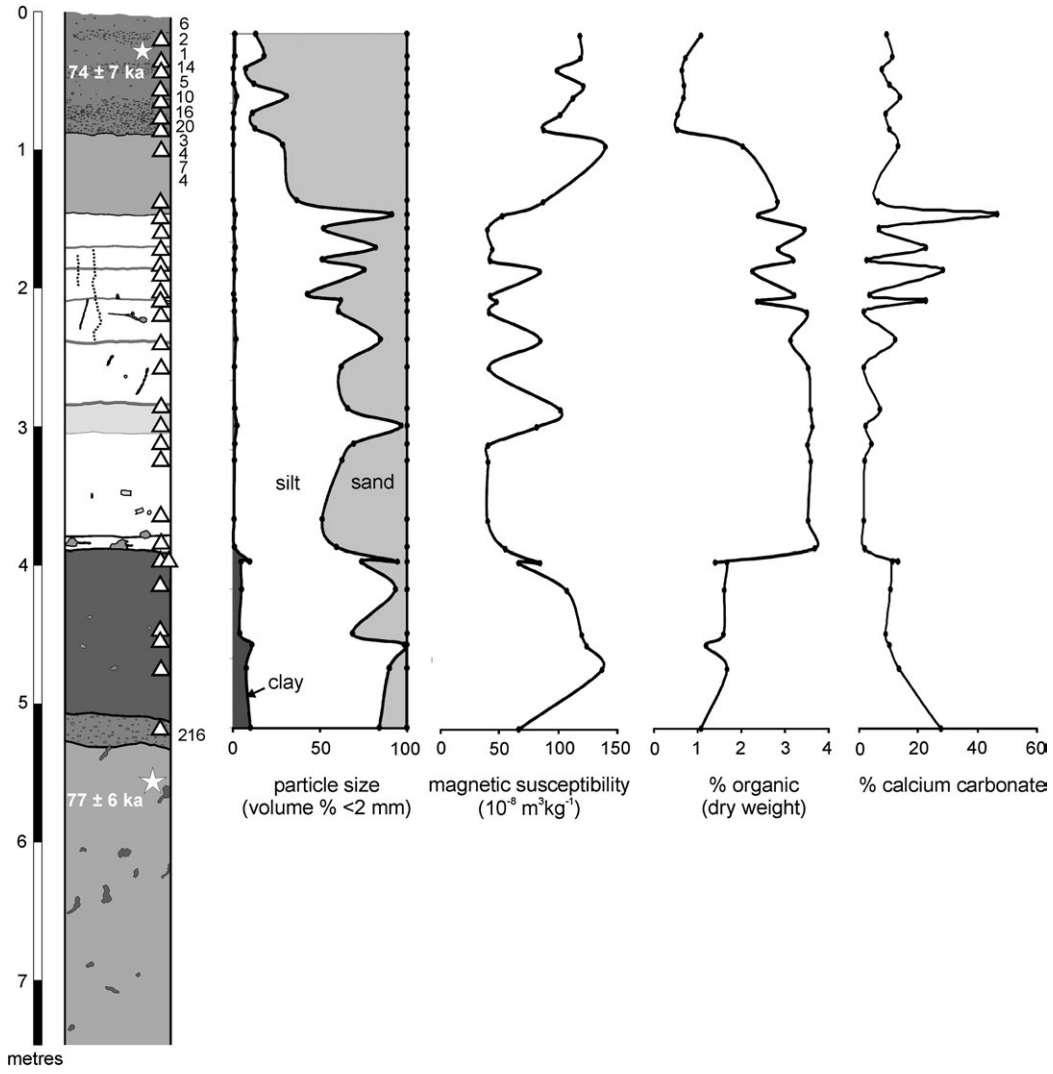

Figure 3. Particle size, magnetic susceptibility, % organic and % calcium carbonate data for sediment samples from the excavated trench at locality 3, Jurreru valley. The location of sediment samples are indicated (triangles), as are the provenance of OSL dates for pre- and post-Toba archaeological contexts (Petraglia et al., 2007). The number and provenance of excavated artefacts are indicated to the left of the profile.

from sedimentological analyses and stratigraphic observations. Phases 1–3 belong to the period prior to the Toba eruption, phase 4 represents the period of ash deposition and redeposition, and phases 5–7 cover the ~30 ka period that post-dates the ash-fall.

Phases 1–3: Pre-Toba environment

Phase 1 is represented by the oldest excavated pre-Toba deposits at locality 3. These comprise ~2.2 m of calcrete-rich clayey silt, dated in its upper levels to 77 ± 6 ka. Phase 2 marked the accumulation of ~0.5 m of silt loam (with ~27% calcium carbonate), which contains numerous lithic artefacts, as well as pebbles and occasional cobbles (Fig. 3). Phase 3 is represented by thick silt loam at locality 3 and by a palaeosol at the Dry Well (artefacts were encountered only in the latter). Phase 3 sediments were buried by up to 2.5 m of YTT at locality 3 during phase 4, while those at the Dry Well were covered by ~60 cm of heavily reworked YTT. The excellent preservation of YTT deposits throughout the valley and certain sedimentological characteristics support the theory that the ash was deposited into a water body. The latter covered at least 0.64 km^2 of the valley at the time of the ash-fall (Petraglia et al., 2007). The data suggest that the area occupied by the water body fluctuated during phases 1–3, with an overall increase in wetness up until the ash-fall. This water body likely consisted of a small and shallow lake or swamp which expanded and contracted according to changes in precipitation and shifts in the rate and extent of fluvial input (Fig. 1B).

The presence of artefacts, pebbles and cobbles within phase 2 sediments at locality 3 and their absence from phase 1 sediments marks a change in environment. A period of aridity at the end of phase 1 is suggested, which resulted in a decrease in the volume of the palaeolake and subsequent exposure of a land surface in the vicinity of the site. Artefacts, manufactured by hominins in the surrounding area, were redeposited together with gravel into the locality 3 area, probably via sheetwash or rills. Depth-associated changes in patterns of patination and edge-rounding on the lithic artefacts suggest that several different phases of artefact transportation and burial may have occurred. A relatively high degree of patination on artefacts redeposited at the end of phase 2 suggests that these artefacts underwent an extended period of surface exposure prior to burial by phase 3 sediments.

An increase in the magnetic susceptibility of the lowermost phase 3 sediments, a slight increase in organic content and no apparent influx of detrital material, all suggest that pedogenesis occurred. A drier episode during this period, or repeated wet–dry intervals, may have resulted in the precipitation of ~27% post-depositional calcium carbonate in phase 2 sediments. In contrast, carbonate levels in phase

https://doi.org/10.1016/j.yqres.2009.11.005 Published online by Cambridge University Press

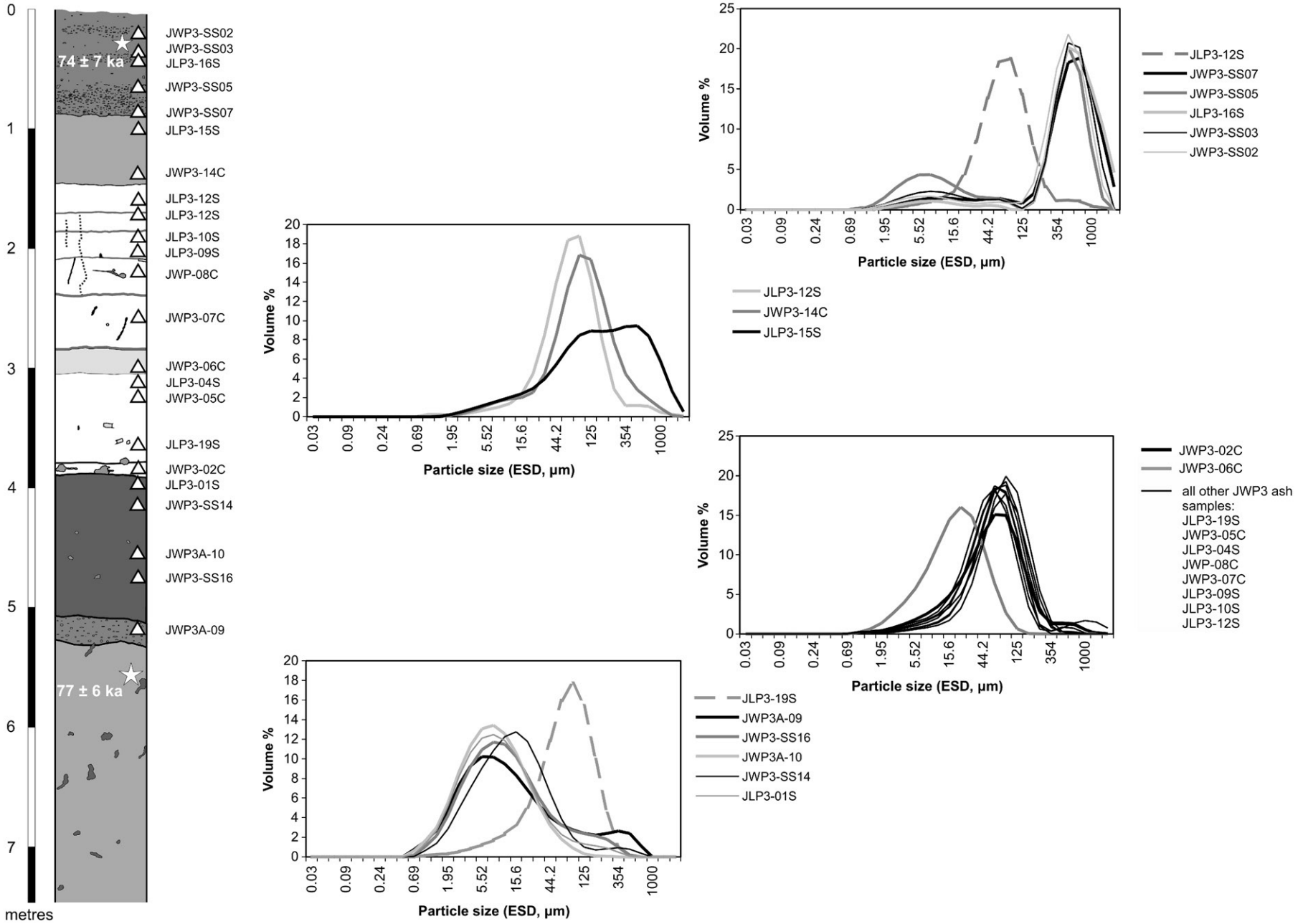

Figure 4. Particle size distributions for sediment and ash samples from locality 3, Jurreru valley.

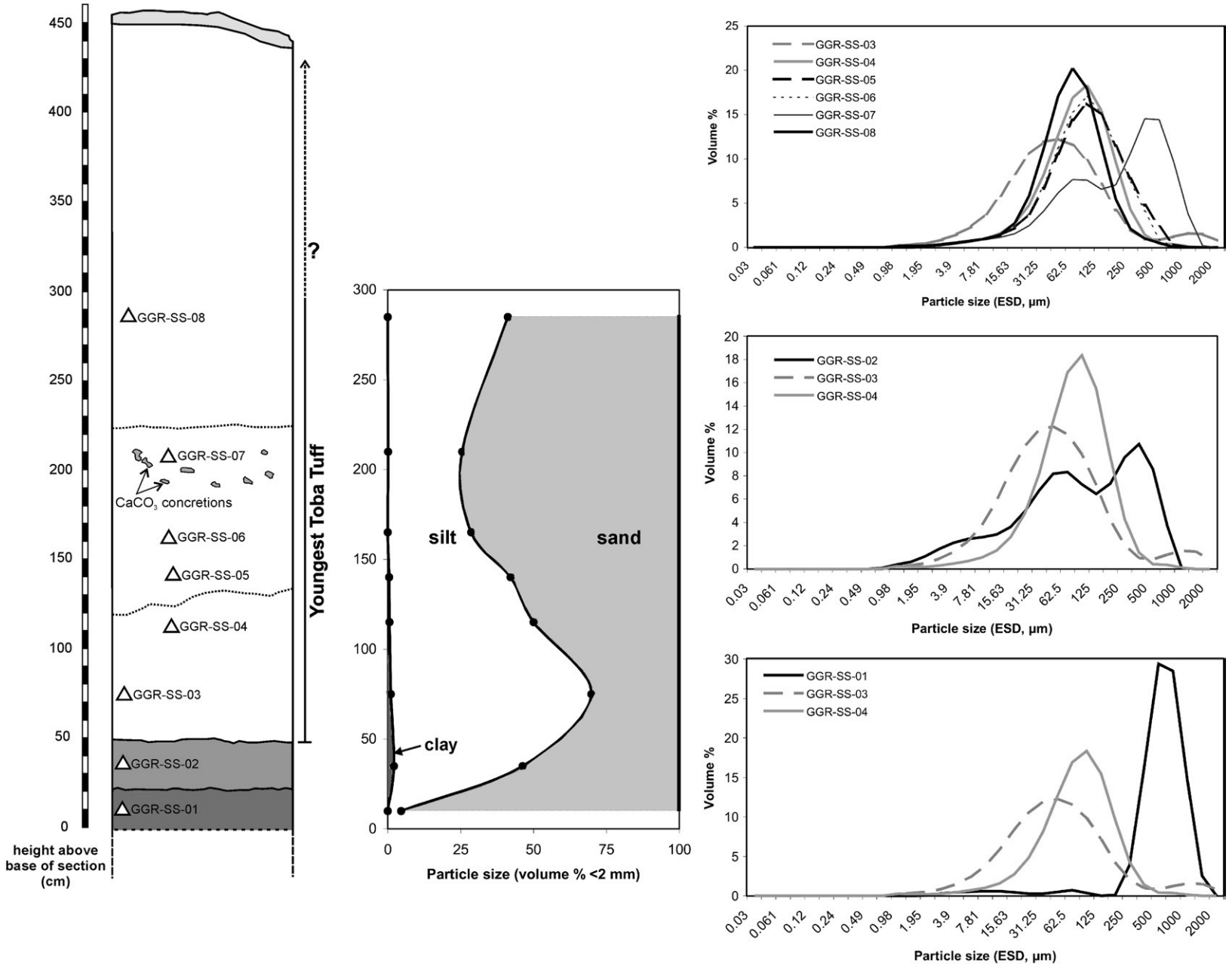

Figure 5. Particle size distributions for sediment and ash samples (triangles) from Ghoghara section, Middle Son valley.

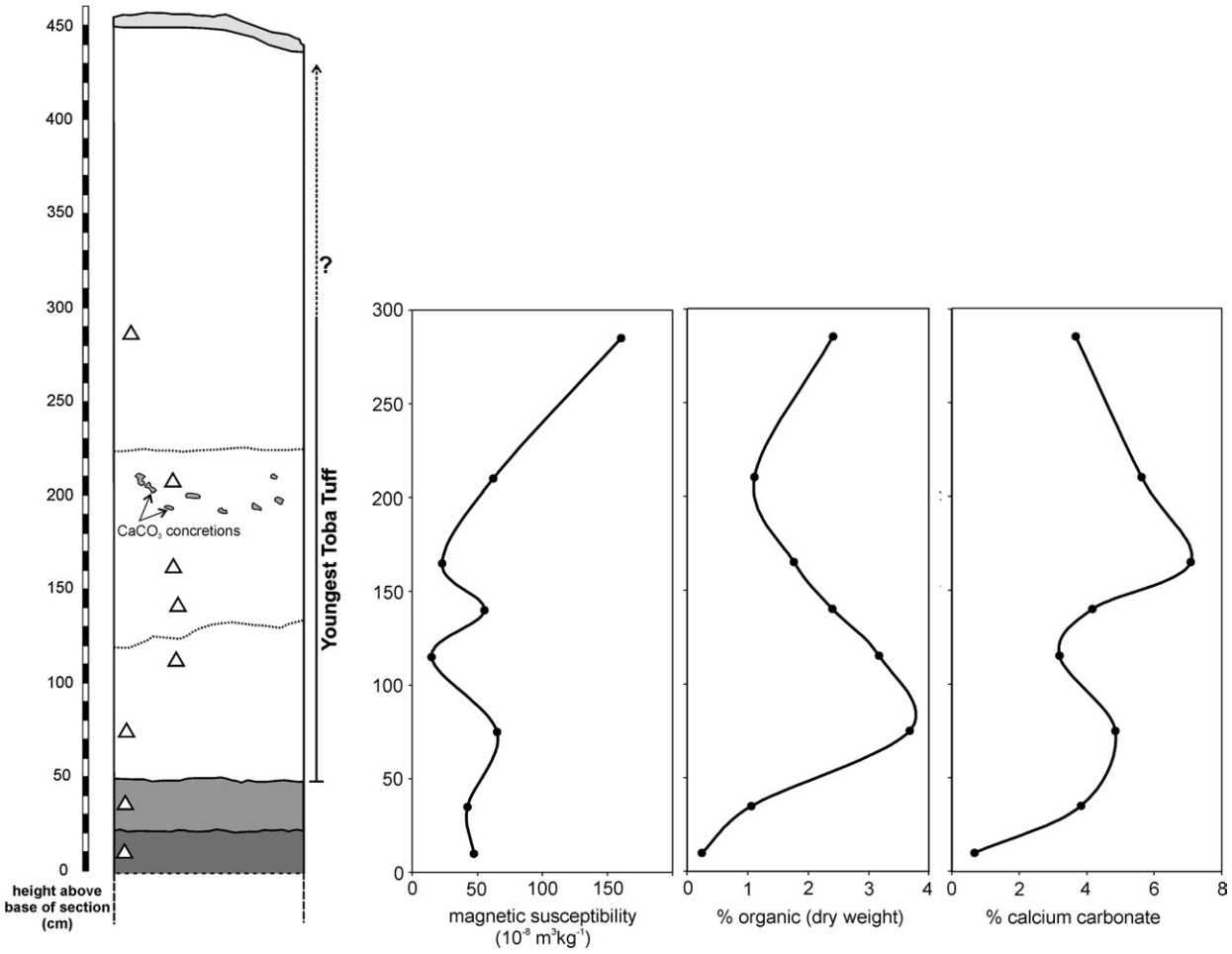

Figure 6. Magnetic susceptibility, % organic and % calcium carbonate data for sediment samples from Ghoghara section.

3 are relatively low, suggestive of an increasingly wet environment during the course of this phase. An upwards decrease in magnetic susceptibility until the Toba ash-fall points to increasingly water-logged conditions and an associated decline in the intensity of pedogenesis. These changes were probably associated with an expansion in the area occupied by the palaeolake. The presence of rhizoliths and an absence of any laminations or bedding structures, normally associated with phases of lacustrine deposition, suggest shallow water conditions. However, bioturbation caused by root growth or burrowing animals could have masked such structures. Past flood events appear to have occurred, represented by at least two phases of input of relatively coarse material into phase 3 deposits; this may have been caused by monsoon-related processes that transported coarser material from the catchment area into the water. Such events would have been localised and short-lived as predominantly silt-sized deposits prevail.

The rate of sediment accumulation during phase 3 was fairly high; the provenance of the OSL date of ~77 ± 6 ka indicates that ~1.8 m of sediment accumulated over a period of ~3 ka. This high rate may have been caused by a combination of strong annual south-west monsoons, bringing water and inorganic material into the valley, and extensive vegetation coverage within and beyond the palaeolake, which introduced additional material. However, organic content of phase 3 sediments is low, not exceeding 1.7%; this may be a result of poor preservation of organic material at this locality. Evidence in support of repeated wetting and drying of the phase 3 deposits, possibly caused by the monsoonal climatic regime, is provided by the mottled colouration of the sediments and overall high magnetic susceptibility values. Orangey brown mottled clay and the presence of black flecks on breakage of peds (Fe–Mn minerals) suggests the presence of redoximorphic features. The palaeosol visible in the Dry Well is broadly equivalent to phase 3 at locality 3, and possibly to phase 2. However, the pre-Toba Dry Well area does not appear to have been submerged by the palaeolake, or was not at the time of the ash-fall as suggested by relatively poor ash preservation at this locality. Instead, the Dry Well may have been situated at or near to the shore-line.

Phase 4: The Toba ash-fall

Close examination of the Jurreru valley's YTT deposits has provided valuable evidence regarding the impact of the ash-fall on the geomorphology and hydrology of the surrounding landscape. On the basis of the internal stratigraphy of the locality 3 ash unit, the accumulation of ash during phase 4 is divided into seven sub-phases of ash deposition. It is argued that the ash was possibly deposited and redeposited into water over at least seven separate events, perhaps over a period of several years. The lowermost ~5 cm of ash represents the only stage of primary deposition (phase 4a), its excellent preservation likely caused by deposition in a calm water environment. All subsequent sub-phases represent periods of ash redeposition. Each horizontal hardpan is argued to mark the termination of a redeposition event, as well as periods of aridity and desiccation prior to successive phases of flooding and ash redeposition in water. The lack of autochthonous terrigenous material in the ash, with the exception of that found in insect burrows and root structures, suggests that redeposition occurred predominantly via aeolian processes rather than by water. The presence of mudcracks within the ash unit supports the theory of wetting and drying cycles, where cracks in the

https://doi.org/10.1016/j.yqres.2009.11.005 Published online by Cambridge University Press

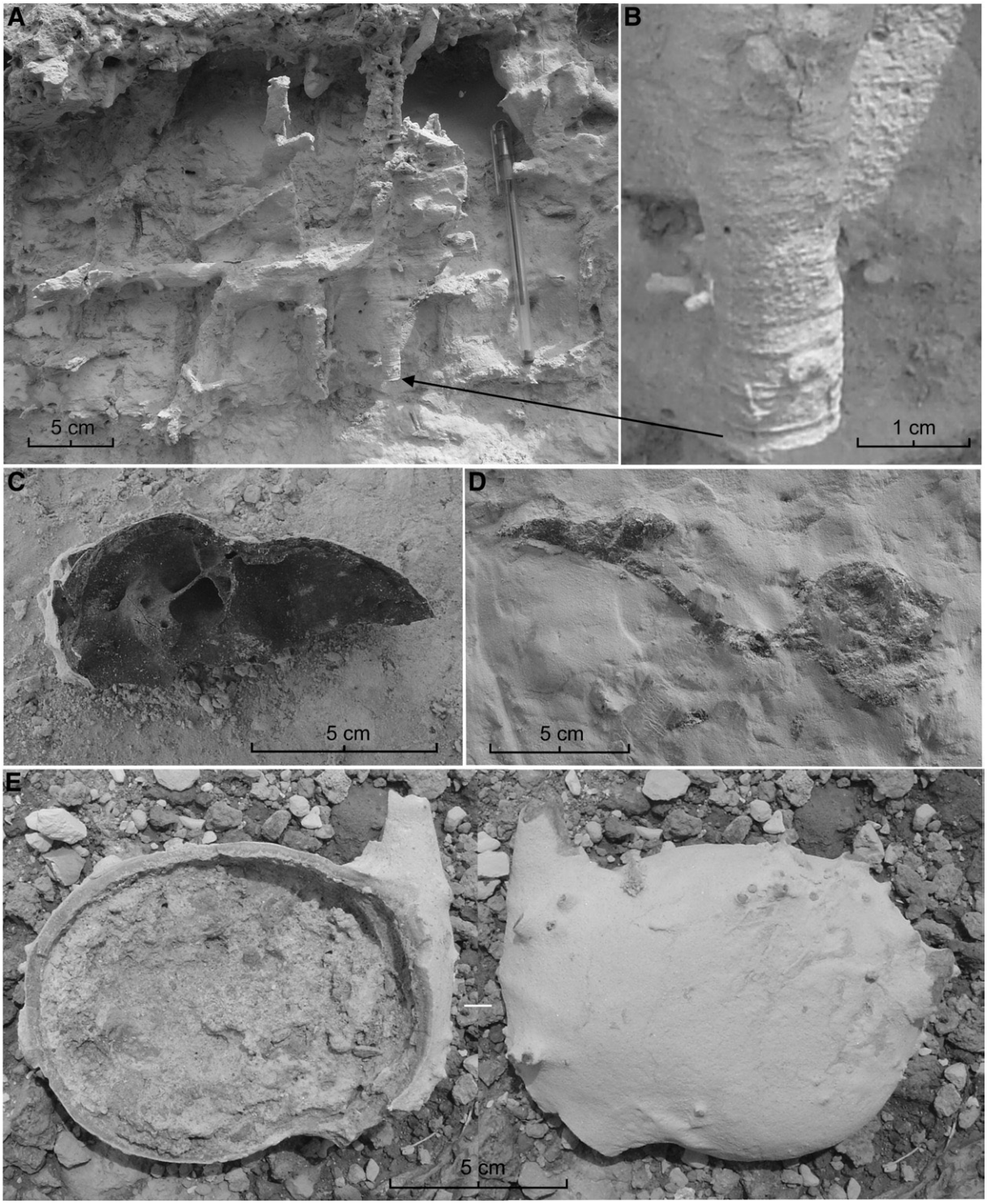

Figure 7. (A, B) *In situ* burrowing structures visible against the weathered section of a mined ash deposit — note the concentric rings in (B); (C) bisected insect chamber (termites?) discovered in one of the ash quarries amongst the heavy fraction of the mining spoil; (D) possible sediment-filled insect burrow, visible in the section walls of the excavated locality 3 trench; (E) fossilized (silicified) termitarium found in the vicinity of locality 3 amongst the heavy fraction of the mining spoil. Internal and external views of the termitarium are to the left and right, respectively.

ash formed during desiccation events that were later filled with fine-grained material during wet episodes. The greatest number of mudcracks derives from the ash surface at the end of phase 4f, probably caused by a hyper-arid period.

Table 2 points out the unique characteristics of each sub-phase; however, several sedimentological features are consistent throughout the ash. The magnetic susceptibility of the ash (mean of 42.5 10^{-8} m^3 kg^{-1}) is consistently low when compared to values for the hardpans and all pre- and post-ash sediments (Fig. 3). All volcanic ash strata are low in carbonate; however, the hardpans possess very high values that increase upwards (the contact between the ash and the ashy sand [phase 5] is comprised of 46% calcium carbonate). Particle size distributions of the nine ash samples are more or less consistent (Fig. 4), and in most samples, the hardpans are composed of finer particles than the ash strata. Fining upwards sequences are particularly apparent at the end of

https://doi.org/10.1016/j.yqres.2009.11.005 Published online by Cambridge University Press

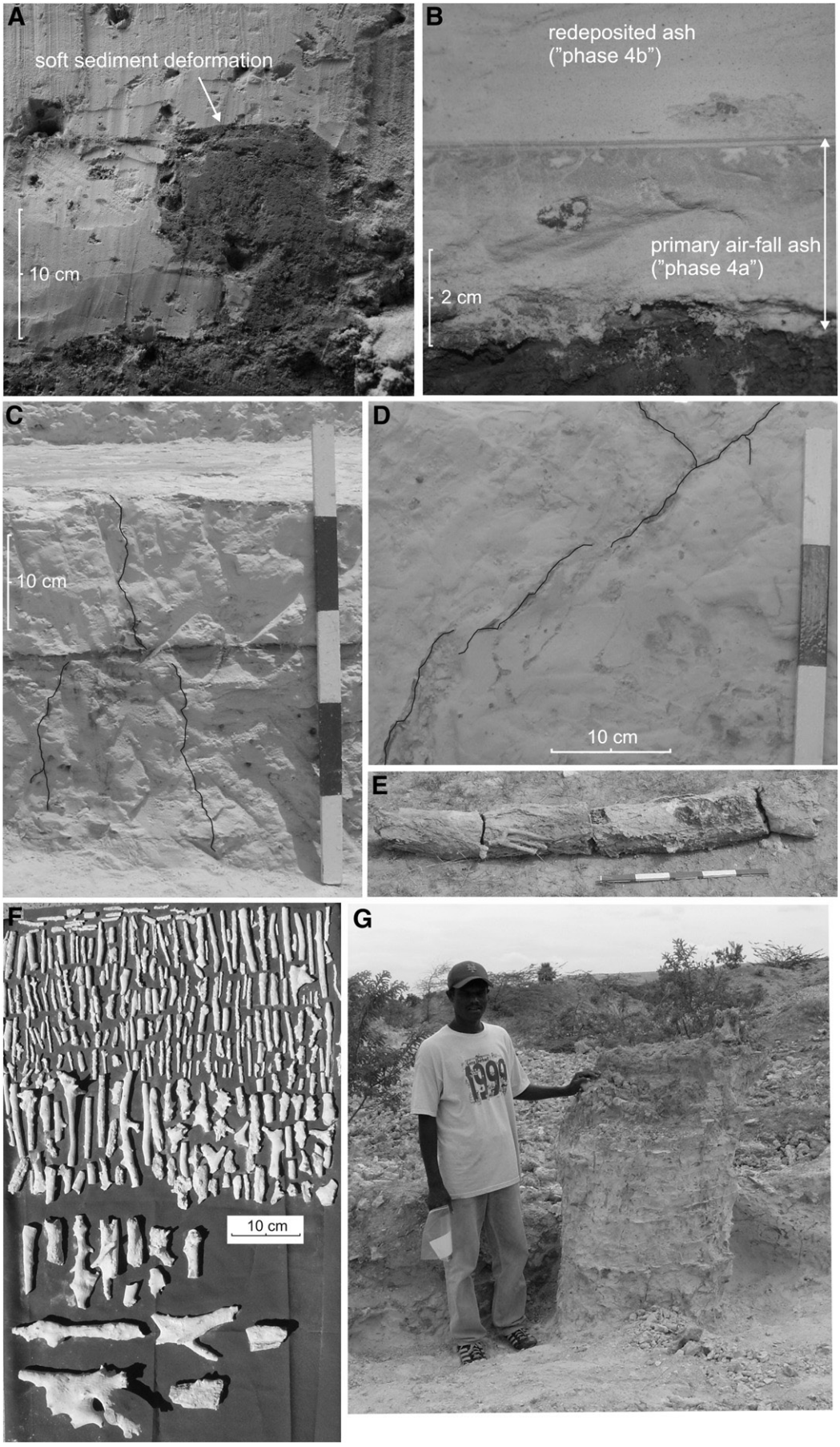

https://doi.org/10.1016/j.yqres.2009.11.005 Published online by Cambridge University Press

Table 2
Phase 4 Toba ash accumulation; characteristics and interpretation of the six sub-phases of ash deposition and redeposition in the Jurreru valley.

Phase	Characteristics
4a	Primary air-fall ash deposition
• Marginally higher magnetic susceptibility (MS) (54.9 10^{-8} m^3 kg^{-1}) than all other ash samples. This could be caused by the presence of a small amount of sediment from phase 3 deposits, visible both within and immediately above the primary ash layer.	
• Contains the highest organic content (3.7%) of all samples from the Jurreru valley as well as the Middle Son.	
• Carbonate content is very low (1.6%).	
• Possesses a more dispersed particle size distribution (PSD), with more fine- and coarse-grained particles in comparison with all other ash strata. In general, however, overall PSD compares closely with that of all other ash strata, where all possess mode values between 44 and 88 μm. Finer material may represent sediment from phase 3 deposits and the coarser material may signal organic matter.	
4b	First ash redeposition and surface pan formation
• The thickest of ash redeposition events buried plant material. This is indicated by the presence of abundant plant fossils that were not discovered in their growth positions during excavation.	
• Fining upwards sequence culminated in a ~10-mm-thick hardpan with dark grey laminations.	
• A sudden increase in MS (81.2 10^{-8} m^3 kg^{-1}) occurs within the finer sediment in the upper levels. This suggests an increase in the presence of relatively fine-grained magnetic minerals, possibly drawn from the surrounding land surface.	
• The surface (hardpan) also exhibits a further increase in MS and cementation with 6.6% carbonate. Cementation may have occurred either before or after phase 4c.	
• After deposition, plants took root and grew across the surface, and animals (perhaps insects, crustaceans, worms, etc.) created tracks and burrows across the surface and into the ash. Occupation of the surface by living organisms could have occurred in a sub-aqueous context, or in a sub-aerial habitat following desiccation of the palaeolake.	
4c	Second ash redeposition and surface pan formation
• A wet episode marked the return of water to the palaeolake.	
• Ash was redeposited probably via aeolian action, burying the surface of the phase 4b pan as well as any organisms growing or living on this surface. Huge quantities of plant material were buried by the ash.	
• The fining-up sequence and hardpan formation is exhibited as in phase 4b. The hardpan is associated with an increase in MS (84.5 10^{-8} m^3 kg^{-1}). Organisms re-occupied the surface, and plants grew upwards from the surface.	
• Desiccation occurred.	
• Before or after burial, the surface of the hardpan became cemented by 12% $CaCO_3$.	
4d	Third ash redeposition and surface pan formation
• Comparable to phase 4c, although a lower density of plant material was buried by the phase 4c ash.	
• Ripples in the ash supports redeposition in water.	
• A minor injection of coarser material perhaps suggests deposition of ash by water as well as wind. However, due to a general absence of clastic material other than ash, redeposition via aeolian processes predominates.	
4e	Fourth ash redeposition and surface pan formation
• Similar to other phases of ash redeposition.	
• $CaCO_3$ content of the hardpan (28%) increased.	
• Density and size of plant fossils and burrows increased.	
4f	Fifth ash redeposition and surface pan formation
• Similar to other phases of ash redeposition.	
• Fossil density and size increased.	
• Extreme period of desiccation marked the end of this redeposition event, as indicated by large mudcracks extending across the surface as well as downwards through the profile.	
• Small plants became established on this surface, where possible evidence of microbial activity is also concentrated.	
4g	Sixth ash redeposition and surface pan formation
• Organic material (3.4%) in the ash increases when compared to the two previous phases.	
• The uppermost few centimetres are composed of material finer than the ash.	
• A substantial period of aridity followed. The surface of the ash became cemented by 46% $CaCO_3$. A degree of carbonate precipitation may have occurred post-burial. In other areas of the valley, this layer forms the ground surface, representing an impenetrable duricrust or petrocalcic horizon, or a combination of both.	
• By the end of this phase, the palaeolake had dried-up, having been plugged by massive quantities of ash. The geomorphology and hydrology of the valley became dramatically altered by the ash-fall and these ash redeposition events. It is plausible that the same lacustrine or palustrine environment that existed in the valley prior to the ash-fall did not return to the valley during the post-Toba period.	

phases 4b, 4c and 4e. The organic content of ash samples is greater than all non-ash samples, with a maximum in the primary ash (3.7%) and a mean value of 3.5% for the redeposited ash. This could be explained by particularly good preservation conditions within the ash, or leaching of humic acids from the palaeolake as the ash settled through water, or the capture and burial of organic matter during redeposition events, possibly following the destruction of organisms by the ash-fall.

During each phase of redeposition, ash from the surrounding landscape was entrained by wind and eventually resettled. A proportion of this ash settled through the water column of the palaeolake. The presence of mudcracks, fossilized plant remains and burrows across the surface of the hardpans support the theory that a period of aridity and desiccation of the palaeolake followed each redeposition event. However, as burrows, tracks and plant structures could also have formed in a sub-aqueous environment, the presence of mudcracks is the main factor supporting the occurrence of desiccation events. Clay- or fine silt-sized minerals in the upper levels of each redeposited ash layer, responsible for a peak in the magnetic susceptibility of the hardpans, may have contained enough nutrients to support the growth of plants or microbes on the surface. This sequence of ash redeposition and regeneration of life on the surface would have been followed by a wet period. During the latter, the palaeolake re-filled with water and more ash was redeposited, succeeded by a period of aridity. This cycle occurred six times at locality 3 and is possibly associated with annual monsoonal cycles.

Figure 8. (A) Soft sediment deformation structures occur at the contact between the ash and the underlying silt loam, suggestive of ash deposition in water; (B) 5-cm-thick probable primary ash-fall at the base of the locality 3 trench — this is overlain by 2.5 m of redeposited ash; (C) mudcracks in section at locality 3 (highlighted with black lines), emanating from the surface of a hardpan and traversing lower hardpans (scale bar = 50 cm); (d) mudcracks (highlighted with black lines) in plan view, visible following exposure of the surface of a hardpan during excavations at locality 3; (E) possible fossilized tree trunk fragments, discovered amongst the heavy fraction of mining spoil (scale bar = 50 cm); (F) all fossils recovered during the excavation of one level at locality 3, amounting to 295 fragments of a variety of sizes that weigh a total of 2.44 kg, equivalent to a fossil density of 19.68 kg m^{-3} — these fossils were recovered from ash that accumulated during the first phase of ash redeposition; (G) possible fossilized tree trunk and/or giant termitarium, located *in situ* in one of the mined ash quarries, where all ash surrounding the structure has been removed by the miners (scale bar = 50 cm).

https://doi.org/10.1016/j.yqres.2009.11.005 Published online by Cambridge University Press

Based on this evidence, it is hypothesized that the redeposited ash may have taken several years to accumulate.

Phase 5

Phase 5 deposits are a characteristic feature of the valley's Quaternary deposits. Comprised of a mixture of YTT and predominantly coarser-grained autochthonous material, this ashy sand layer is encountered throughout the Jurreru valley. At locality 3, the volcanic ash content of the ashy sand decreased towards the end of phase 5, associated with an upwards increase in magnetic susceptibility and decrease in organic content; a similar pattern is evident in the Dry Well deposits. The upwards decrease in organic matter perhaps marked a decline in optimal conditions for organic preservation, caused by an increasingly low ash content. Alternatively, clearance of organic matter from a large proportion of the landscape by the end of phase 5 may be invoked. In this case, a stark and unvegetated landscape perhaps existed in areas affected by the ash-fall. The mixing of ash and coarser sediment implies deposition by water rather than wind; perhaps via sheetwash and rill erosion of the surrounding hill slopes and ground surface, with devegetation contributing to increased rates of erosion. Low-energy deposition is suggested because pebble-sized clasts rarely occur. This phase marks the return of hominins to the valley after a hiatus in occupation, shown by a lack of artefacts from within the ash or the lower levels of phase 5 deposits. However, the duration of this hiatus was not substantial, indicated by the provenance of the 74 ± 7 ka OSL date from phase 6 deposits at locality 3.

Phase 6

At locality 3, phase 6 deposits extend from above the ashy sand to the ground surface, where lithic artefacts are present throughout. Organic content is consistently low with only minor changes. Carbonate content fluctuates in concert with particle size, where the former increases as the proportion of silt increases. Magnetic susceptibility fluctuates during phase 6, and although texture alternates between sand, sandy loam and loamy sand, the particle size distributions of all samples are consistent (Fig. 4). There are no deep cut and fill events but there are lenses of variable sediments, suggestive of gentler forms of erosion and deposition rather than channel formation. This implies a predominance of flood events that eroded and redeposited material over the surface rather than stream or riverine activity in this area. A lack of evidence of soil formation processes suggests that unstable land surfaces existed. Instead, continued processes of erosion and redeposition are supported by the presence of discrete pebble- or cobble-sized aggregated grey ash and ashy sand within phase 6 sediments. Phase 6 marks the return of wetter conditions to the valley, and because these sediments are dated to 74 ± 7 ka, it is hypothesized that this phase coincides with interstadial D-O 19.

Phase 7

The earliest phase 7 deposits are encountered at locality 21, dated to 38 ± 3 ka (Petraglia et al., 2009). Therefore, there currently exists a temporal gap of ~30 ka in between phases 6 and 7; perhaps the intervening deposits exist but have yet to be encountered, or aggradation ceased in the valley during this period. In both cases, phases of palaeoenvironmental change in between phases 6 and 7 remain to be described. This temporal gap partially coincides with OIS 4, a period when a weakened south-west monsoonal system existed in India, causing aridity in certain areas (e.g., Prabhu et al., 2004). During this period, aridity in the Jurreru valley may have led to reduced or a cessation of fluvial activity, as well as deposition and soil formation processes. The lower two sediment samples from locality 21 are predominantly comprised of YTT. The next sample in the sequence shows a peak in clay and fine silt-sized particles but also contains a significant proportion of ash; this sample shares its provenance with the OSL date of 38 ± 2 ka and also shows an increase in magnetic susceptibility and carbonate content. The ash likely acted as the parent material for pedogenesis; therefore, the earliest phase 7 deposits marked the beginning of soil formation. This was later curtailed by episodes of erosion and aggradation (indicated by an increase in both magnetic susceptibility and the input of coarser particles), possibly corresponding with flood events. The middle part of phase 7 marks a further increase in cut and fill episodes, flood events and coarse material accumulation at locality 21, perhaps indicative of increased wetness and monsoonal strength.

Before the Toba eruption, the hydrology of the Jurreru valley was dominated by a lacustrine or palludal environment, probably fed by small rivers. After Toba, this water body was plugged by volcanic ash, dramatically affecting the valley's geomorphology and hydrology. Because of the increased wetness suggested for this period, it is possible that the modern Jurreru river began to carve a course through the valley during phase 7. This probably coincides with OIS 3, a period when increased humidity and stronger summer south-west monsoons existed in India (e.g., Rajagopalan et al., 1997; Srivastava et al., 2003). During later periods of phase 7, soil formation in several regions of the valley took place. This is supported by sedimentological data from locality 21 and visible vertisols at several other localities. Noticeable increases in vegetation coverage and land surface stability are also posited, in stark comparison with earlier post-Toba phases when a more barren landscape is invoked.

Toba ash redeposition in the Middle Son valley

At Ghoghara, a change from a high energy to low energy depositional environment prior to the ash-fall is suggested by a shift from moderately well sorted sand to very poorly sorted sandy loam in the 50 cm of pre-Toba deposits. The excellent preservation of the ash, its discontinuous exposure in the cliff section, and the slight increase in organic matter in the uppermost pre-Toba deposits all suggest that the ash was redeposited into a water-filled channel where relatively anaerobic conditions prevailed. The evidence at Khuteli also indicates that the ash was redeposited into a former channel. A hydrologically active and wet environment likely existed in these areas of the valley before the ash-fall.

At least six phases of ash redeposition are evident at Ghoghara. Fluctuating magnetic susceptibility suggests varying input of detrital material (magnetic minerals) during redeposition (Fig. 6). This may signal separate ash redeposition events where ash was transported from different source regions. The proportion of sand within the ash steadily increases upwards with the exception of the uppermost sample. The lowermost ash sample is surprisingly fine-grained when compared to all other ash samples; microscopic examination indicates that this sample is composed of particularly fine-grained glass shards, considerably finer that all other ash samples from both the Middle Son and Jurreru. This discrepancy could signal relatively intensive weathering of shards, or sorting of the ash into a fine fraction during gentle redeposition into an aqueous environment, or aeolian deposition where wind energy was only sufficient to entrain the finest ash particles before deposition.

The next three ash samples in the sequence show similar particle size distributions but with an increase through time in the coarser fraction. The penultimate sample shows a notable difference from previous ash samples, possessing a roughly bimodal distribution that indicates the presence of ash but a predominance of medium sand (Fig. 5). The context of this sample marks the approximate position of an erosional ledge, which itself denotes a textural change in the sediment profile. The uppermost ash sample

https://doi.org/10.1016/j.yqres.2009.11.005 Published online by Cambridge University Press

is particularly noteworthy, marking an increase in organic content, magnetic susceptibility and a late influx of ash-rich sediment when compared to the relatively ash-poor underlying sample. The strong peak in magnetic susceptibility reflects an influx of magnetic materials and given that this sample contains a significant proportion of YTT, which possesses a relatively low magnetic susceptibility, this high value suggests that the geographic source of this later reworked ash was different from that of the underlying ash. This evidence indicates that ash in the valley was being redeposited for some time after the eruption, over several separate cycles of redeposition, with the ash being derived from different source areas.

As with the Jurreru ash samples, organic content peaks at the base of the ash at both Ghoghara and Khuteli. At Ghoghara, this decreases steadily as the amount of sand in the reworked ash increases. Again, this pattern may reflect either better preservation of organic material in volcanic ash, or entrapment of organic matter within the ash as it was being deposited. Carbonate-content fluctuates throughout the ash and the presence of carbonate concretions in the ash at Ghoghara as well as at Khuteli suggests environmental aridity at some stage after the eruption.

The Toba ash-fall probably post-dates the accumulation of the Patpara formation (Williams and Royce, 1982; Basu et al., 1987; Acharyya and Basu, 1993; Jones and Pal, 2005, 2009; but see Williams et al., 2006), when a braided river system is argued to have existed in the valley (Sharma and Clark, 1983). Following the ash-fall, aeolian processes could have transported ash from the valley and surrounding hills into areas of topographic depression. Such areas would include any channels, tributaries or isolated pools. After entrainment via either water or wind, the ash would have choked these areas during successive periods of ash redeposition. The aggradation of the massive Baghor formation sediments that dominate the geomorphology of the valley today either post-dated the Toba ash-fall (Williams and Clarke, 1995) or had commenced shortly beforehand (Acharrya and Basu, 1993). *In situ* carbonate-cemented sands structures, diagnostic of the Baghor coarse member (Williams and Royce, 1982), are visible directly above the ash at Khuteli (Jones and Pal, 2005). It is proposed that a change in depositional regime in the Middle Son valley, marked by the onset of the aggradation of coarse Baghor formation sediments, occurred following both the ash-fall and a lengthy period of aridity in the valley that was possibly coincident with OIS 4; this is consistent with IRSL dates for Baghor formation contexts (Williams et al., 2006). In fact, the onset of periods of loess deposition in China ~71 ka (An et al., 1991; Huang et al., 2001) and in Pakistan ~74 ka (Dennell et al., 1992) represents evidence of a post-Toba shift in Asian monsoonal dynamics, where the summer south-west monsoon weakened and the winter northeast monsoon strengthened. This would have resulted in increased aridity in areas of northern India in particular, supported by marine core evidence from the Bay of Bengal and Arabian Sea that indicates decreased fluvial input during this period (Kudrass et al., 2001; von Rad et al., 2002). Therefore, arid conditions and drought likely persisted in the Middle Son valley during both OIS 4 and the stadial in between D-O 19 and 20, having been caused by a depressed south-west monsoon and significantly stronger north-east monsoon.

Determining how long it took for the ash to be redeposited and consolidated or buried in both the Jurreru and Middle Son valleys is critical for understanding the duration and severity of its environmental impact; the longer the ash remained mobile in the environment, the more chronic the impact on vegetation and animal and human health. Several previous studies, often focused on recent historical eruptions, have discussed processes of tephra deposition, redistribution and redeposition. After the initial deposition of ash following the eruption of the Hudson volcano in Chile in 1991, strong winds were shown to have redistributed vast amounts of tephra during a week-long period (Scasso et al., 1994). Following examination of a 10-Ma rhyolitic ash-fall in Nebraska (Voorhies and Thomasson, 1979), Rose et al. (2003) note substantial thickening of ash deposits via water and/or wind, albeit favouring aeolian redistribution. Abundant air-borne ash is posited to have persisted for several months or more following initial deposition. Watt et al. (2009) examined the redistribution of ash following the eruption of Chaitén in Chile in 2008, where wind and rain were responsible for the erosion and redeposition of the primary ash layer into secondary thicker deposits. After revisiting ash-fall sites seven months later, water run-off proved to be the principal process that remobilised the ash deposits. However, other sites, where ash thicknesses had been greater than a few millimetres, remained remarkably unchanged. Crusting of the surface of the ash after a wetting then drying episode, as well as stabilisation of the ash through plant growth, are both argued to have rendered the ash relatively resistant to erosion. In contrast, Rees (1979) studied the physiographic effects of ash following the Parícutin eruption (Mexico, 1943) and discovered that ash was still mobile, particularly on plains, 30 yr after the eruption. The unconsolidated ash was easily eroded, transported and redeposited, particularly during the rainy season. Less vigorous erosional processes persisted for years via soil creep, landslides, sheet flow, wind deflation, and splash, rill and channel erosion (Rees, 1979). In summary, some studies indicate that ash can be redeposited relatively soon after the initial ash-fall, whereas others show that ash can remain mobile in the environment for a substantial period of time. In this study, evidence from the Jurreru and Middle Son valleys suggests that the majority of the ash took at least several years to be redeposited. In the Jurreru, YTT continued to be redistributed during “phase 5” and, to a lesser extent, during “phase 6,” at least hundreds of years after the eruption.

Conclusion

This represents the first study to investigate the environmental consequences of the Toba eruption in two river valleys in India, separated by a distance of ~1100 km. Because of the types of sedimentological analyses employed, the interpretations presented here focus predominantly on the geomorphological consequences of the ash-fall, such as changes in landscape and local hydrological systems. Substantial landscape remodelling appears to have occurred in both valleys after the Toba ash-fall, where a succession of separate phases of ash redeposition occurred, culminating in thick deposits of reworked ash. These processes probably resulted in a decline in vegetation coverage and cessation of pedogenesis. In addition, water sources and plants may have become toxic if leaching of heavy metals and fluorine contained within and adhering to the volcanic glass took place (e.g., Witham et al., 2005). This may have proved hazardous for grazing animals and hominin populations. Under normal conditions, the river valleys would have been attractive areas for both animals and hominins for food resources, water, and sources of lithic materials for artefact manufacture. On a broader geographic scale, the Jurreru and Middle Son valleys are only two small areas affected by the Toba ash-fall; distal YTT covered a large area of peninsular India and the processes described here may have been repeated throughout the subcontinent. Given the diverse range of habitats and micro-climates that exist throughout India, in conjunction with topographic variability determining the rapidity with which ash was removed from the landscape and buried, it is probable that the Toba eruption had highly variable impacts throughout India. Geographical variability in post-Toba habitat disruption and fragmentation, caused by both the ash-fall and climate change, likely resulted in considerable spatial variability in hominin responses to the ash-fall. A heterogeneity in the extent to which hominin populations survived the Toba eruption is suggested, with some areas of India left worse-affected than others.

https://doi.org/10.1016/j.yqres.2009.11.005 Published online by Cambridge University Press

Acknowledgments

This research was funded by Newnham College, the Faculty of Archaeology and Anthropology (University of Cambridge), the Prehistoric Society, and the Society of Antiquaries of London. Fieldwork in the Middle Son was conducted with J.N. Pal, M.C. Gupta and R. Prasad. Research in the Jurreru valley was conducted by an international team under the direction of M. Petraglia and R. Korisettar and was funded by NERC, the Leakey Foundation, the ARC, and the McDonald Institute for Archaeological Research. I thank C. Oppenheimer and P. Ditchfield for discussions regarding the Jurreru evidence, R. Roberts for OSL dates, and the two anonymous reviewers who commented on an earlier draft. The help of S. Boreham, C. Clarkson, L. Farr, D. Pyle, C. Rolfe and C. Shipton is gratefully acknowledged.

Appendix A. Supplementary data

Supplementary data associated with this article can be found, in the online version, at doi:10.1016/j.yqres.2009.11.005.

References

Acharyya, S.K., Basu, P.K., 1993. Toba ash on the Indian subcontinent and its implications for correlation of Late Pleistocene alluvium. Quaternary Research 40, 10–19.
Ambrose, S.H., 1998. Late Pleistocene human populations bottlenecks, volcanic winter, and differentiation of modern humans. Journal of Human Evolution 34, 623–651.
An, Z., Kukla, G., Porter, S.C., Xiao, J., 1991. Magnetic susceptibility evidence of monsoon variation on the loess plateau of Central China during the last 130,000 years. Quaternary Research 36, 26–29.
Basu, P.K., Biswas, S., Acharyya, S.K., 1987. Late Quaternary ash beds from Son and Narmada basins, Madhya Pradesh. Indian Minerals 41, 66–72.
Bekki, S., Pyle, J.A., Zhong, W., Toumi, R., Haigh, J.D., Pyle, D.M., 1996. The role of microphysical and chemical processes in prolonging the climate forcing of the Toba eruption. Geophysical Research Letters 23, 2669–2672.
Bühring, C., Sarnthein, M., Party, Leg 184 Shipboard Scientific Party, 2000. Toba ash layers in the South China Sea: evidence of contrasting wind directions during eruption ca. 74 ka. Geology 28, 275–278.
Chesner, C.A., Rose, W.I., 1991. Stratigraphy of the Toba Tuffs and the evolution of the Toba Caldera Complex, Sumatra, Indonesia. Bulletin of Volcanology 53, 343–356.
Cronin, S.J., Hedley, M.J., Neall, V.E., Smith, R.G., 1998. Agronomic impact of tephra fallout from the 1995 and 1996 Ruapehu volcano eruptions, New Zealand. Environmental Geology 34, 21–30.
Dale, V.H., Delgado-Acevedo, J., MacMahon, J., 2005. Effects of modern volcanic eruptions on vegetation. In: Martí, J., Ernst, G.G.J. (Eds.), Volcanoes and the environment. Cambridge Univ. Press, Cambridge, pp. 227–249.
Dennell, R.W., Rendell, H.M., Halim, M., Moth, E., 1992. A 45-000-year-old open-air Paleolithic site at Riwat, northern Pakistan. Journal of Field Archaeology 19, 17–33.
Gathorne-Hardy, F., Harcourt-Smith, W., 2003. The super-eruption of Toba, did it cause a human bottleneck? Journal of Human Evolution 45, 227–230.
Grattan, J., 2006. Aspects of Armageddon: an exploration of the role of volcanic eruptions in human history and civilization. Quaternary International 151, 10–18.
Gu, L., Baldocchi, D.D., Wofsy, S.C., Munger, J.W., Michalsky, J.J., Urbanski, S.P., Boden, T.A., 2003. Response of a deciduous forest to the Mount Pinatubo eruption: enhanced photosynthesis. Science 299, 2035–2038.
Horwell, C.J., Baxter, P.J., 2006. The respiratory health hazards of volcanic ash: a review for volcanic risk mitigation. Bulletin of Volcanology 69, 1–24.
Huang, C.-Y., Zhao, M., Wang, C.-C., Wei, G., 2001. Cooling of the South China Sea by the Toba eruption and correlation with other climate proxies ~71,000 years ago. Geophysical Research Letters 28, 3915–3918.
Jones, G.S., Gregory, J.M., Stott, P.A., Tett, S.F.B., Thorpe, R.B., 2005. An AOGCM simulation of the climate response to a volcanic super-eruption. Climate Dynamics 25, 725–738.
Jones, M.T., Sparks, R.S.J., Valdes, P.J., 2007. The climatic impact of supervolcanic ash blankets. Climate Dynamics 29, 553–564.
Jones, S.C., 2007a. The Toba supervolcanic eruption: tephra-fall deposits in India and palaeoanthropological implications. In: Petraglia, M.D., Allchin, B. (Eds.), The evolution and history of human populations in South Asia. Springer/Kluwer Academic Publishers, New York, pp. 173–200.
Jones, S.C., 2007b. A human catastrophe? The impact of the ~74,000 year-old supervolcanic eruption of Toba on hominin populations in India. PhD thesis, University of Cambridge, England.
Jones, S.C., Pal, J.N., 2005. The Middle Son valley and the Toba supervolcanic eruption of 74 kyr BP: Youngest Toba Tuff deposits and Palaeolithic associations. Journal of Interdisciplinary Studies in History and Archaeology 2, 47–62.
Jones, S.C., Pal, J.N., 2009. The Palaeolithic of the Middle Son valley, north-central India: changes in hominin lithic technology and behaviour during the Upper Pleistocene. Journal of Anthropological Archaeology 28, 323–341.
Kudrass, H.R., Hofmann, A., Doose, H., Emeis, K., Erlenkeuser, H., 2001. Modulation and amplification of climatic changes in the Northern Hemisphere by the Indian summer monsoon during the past 80 k.y. Geology 29, 63–66.
Mason, B.G., Pyle, D.M., Oppenheimer, C., 2004. The size and frequency of the largest explosive eruptions on Earth. Bulletin of Volcanology 66, 735–748.
Ninkovich, D., Sparks, R.S.J., Ledbetter, M.T., 1978. The exceptional magnitude and intensity of the Toba eruption, Sumatra: an example of the use of deep-sea tephra layers as a geological tool. Bulletin Volcanologique 41, 286–298.
Oppenheimer, C., 2002. Limited global change due to the largest known Quaternary eruption, Toba 74 kyr BP. Quaternary Science Reviews 21, 1593–1609.
Pattan, J.N., Shane, P., Banakar, V.K., 1999. New occurrence of Youngest Toba Tuff in abyssal sediments of the Central Indian Basin. Marine Geology 155, 243–248.
Petraglia, M., Korisettar, R., Boivin, N., Clarkson, C., Ditchfield, P., Jones, S., Koshy, J., Lahr, M.M., Oppenheimer, C., Pyle, D., Roberts, R., Schwenninger, J.-L., Arnold, L., White, K., 2007. Middle Paleolithic assemblages from the Indian Subcontinent before and after the Toba Super-Eruption. Science 317, 114–116.
Petraglia, M., Korisettar, R., Kasturi Bai, M., Boivin, N., Janardhan, B., Clarkson, C., Cunningham, K., Ditchfield, P., Fuller, D., Hampson, J., Haslam, M., Jones, S., Koshy, J., Miracle, P., Oppenheimer, C., Roberts, R., White, K., 2009. Human occupation, adaptation and behavioral change in the Pleistocene and Holocene of South India: recent investigations in the Kurnool District, Andhra Pradesh. Eurasian Prehistory 6 (1–2), 119–166.
Prabhu, C.N., Shankar, R., Anupama, K., Taieb, M., Bonnefille, R., Vidal, L., Prasad, S., 2004. A 200-ka pollen and oxygen-isotopic record from two sediment cores from the eastern Arabian Sea. Palaeogeography, Palaeoclimatology, Palaeoecology 214, 309–321.
Rajagopalan, G., Sukumar, R., Ramesh, R., Pant, R.K., Rajagopalan, G., 1997. Late Quaternary vegetational and climatic changes from tropical peats in southern India — an extended record up to 40,000 years BP. Current Science 73, 60–63.
Rampino, M.R., Self, S., 1992. Volcanic winter and accelerated glaciation following the Toba super-eruption. Nature 359, 50–52.
Rees, J.D., 1979. Effects of the eruption of Parícutin volcano on landforms, vegetation, and human occupancy. In: Sheets, P., Grayson, D.K. (Eds.), Volcanic Activity and Human Ecology. Academic Press, New York, pp. 249–292.
Riedel, J.L., Pringle, P.T., Schuster, R.L., 2001. Deposition of Mount Mazama tephra in a landslide-dammed lake on the upper Skagit River, Washington, USA. In: White, J.D. L., Riggs, N.R. (Eds.), Volcaniclastic sedimentation in lacustrine settings. Blackwell Science, U.K., pp. 285–298.
Robock, A., Ammann, C.M., Oman, L., Sindell, D., Levis, S., Stenchikov, G., 2009. Did the Toba volcanic eruption of ~74 ka B.P. produce widespread glaciation? Journal of Geophysical Research 114, D10107.
Rose, W.I., Chesner, C.A., 1987. Dispersal of ash in the great Toba eruption, 75 ka. Geology 15, 913–917.
Rose, W.I., Riley, C.M., Darteville, S., 2003. Size and shapes of 10-Ma distal fall pyroclasts in the Ogallala Group, Nebraska. Journal of Geology 111, 115–124.
Scasso, R.A., Corbella, H., Tiberi, P., 1994. Sedimentological analysis of the tephra from the 12-15 August 1991 eruption of Hudson volcano. Bulletin of Volcanology 56, 121–132.
Schulz, H., Emeis, K.-C., Erlenkeuser, H., von Rad, U., Rolf, C., 2002. The Toba volcanic event and interstadial/stadial climates at the marine isotopic stage 5 to 4 transition in the Northern Indian Ocean. Quaternary Research 57, 22–31.
Self, S., 2006. The effects and consequences of very large explosive volcanic eruptions. Philosophical Transactions of the Royal Society A 364, 2073–2097.
Sharma, G.R., Clark, J.D., 1983. Palaeoenvironments and prehistory in the Middle Son Valley. Abinash Prakashan, Allahabad.
Sparks, S., Self, S., Grattan, J., Oppenheimer, C., Pyle, D., Rymer, H., 2005. Super-eruptions: global effects and future threats. Report of a Geological Society of London Working Group. The Geological Society, London, p. 123.
Srivastava, P., Singh, I.B., Sharma, M., Singhvi, A.K., 2003. Luminescence chronometry and Late Quaternary geomorphic history of the Ganga Plain, India. Palaeogeography, Palaeoclimatology, Palaeoecology 197, 15–41.
von Rad, U., Burgath, K.-P., Pervaz, M., Schulz, H., 2002. Discovery of the Toba ash (c. 70 ka) in a high-resolution core recovering millennial monsoonal variability off Pakistan. In: Clift, P.D., Kroon, D., Gaedicke, C., Craig, J. (Eds.), The tectonic and climatic evolution of the Arabian Sea region. Geological Society Special Publication No. 195. The Geological Society, London, pp. 445–461.
Voorhies, M., Thomasson, J.R., 1979. Fossil grass anthoecia within Miocene rhinoceros skeletons: diet in an extinct species. Science 206, 331–333.
Watt, S.F.L., Pyle, D.M., Mather, T.A., Martin, R.S., Matthews, N.E., 2009. Fallout and distribution of volcanic ash over Argentina following the May 2008 explosive eruption of Chaitén. Chile. Journal of Geophysical Research 114, B04207.
Westgate, J.A., Shane, P.A.R., Pearce, N.J.G., Perkins, W.T., Korisettar, R., Chesner, C.A., Williams, M.A.J., Acharyya, S.K., 1998. All Toba tephra occurrences across Peninsular India belong to the 75,000 yr B.P. eruption. Quaternary Research 50, 107–112.
Williams, M.A.J., Clarke, M.F., 1995. Quaternary geology and prehistoric environments in the Son and Belan valleys, North Central India. In: Wadia, S., Korisettar, R., Kale, V.S. (Eds.), Quaternary environments and geoarchaeology of India. Geological Society of India, Bangalore, pp. 282–308.
Williams, M.A.J., Royce, K., 1982. Quaternary geology of the Middle Son valley, North Central India: implications for prehistoric archaeology. Palaeogeography, Palaeoclimatology, Palaeoecology 38, 139–162.
Williams, M.A.J., Pal, J.N., Jaiswal, M., Singhvi, A.K., 2006. River response to Quaternary climatic fluctuations: evidence from the Son and Belan valleys, north-central India. Quaternary Science Reviews 25, 2619–2631.
Witham, C.S., Oppenheimer, C., Horwell, C.J., 2005. Volcanic ash-leachates: a review and recommendations for sampling methods. Journal of Volcanology and Geothermal Research 141, 299–326.
Zielinski, G.A., Mayewski, P.A., Meeker, L.D., Whitlow, S., Twickler, M., Taylor, K., 1996. Potential atmospheric impact of the Toba mega-eruption ~71,000 years ago. Geophysical Research Letters 23, 837–840.